The Journal of Immunology

Roles of the Ig κ Light Chain Intronic and 3′ Enhancers in *Igk* Somatic Hypermutation

Matthew A. Inlay, Heather H. Gao, Valerie H. Odegard, Tongxiang Lin, David G. Schatz and Yang Xu

J Immunol 2006; 177:1146-1151; ;
doi: 10.4049/jimmunol.177.2.1146
http://www.jimmunol.org/content/177/2/1146

The Journal of Immunology is published twice each month by
The American Association of Immunologists, Inc.,
1451 Rockville Pike, Suite 650, Rockville, MD 20852

Print ISSN: 0022-1767 Online ISSN: 1550-6606.

Roles of the Ig κ Light Chain Intronic and 3′ Enhancers in *Igk* Somatic Hypermutation[1]

Matthew A. Inlay,[2]* Heather H. Gao,[2]* Valerie H. Odegard,[†] Tongxiang Lin,* David G. Schatz,[†] and Yang Xu[3]*

Somatic hypermutation (SHM) of the rearranged Ig genes is required for the affinity maturation of Abs. SHM is almost exclusively targeted to the rearranged Ig loci, but the mechanism of this gene-specific targeting remains unclear. The Ig κ L chain locus contains multiple enhancers, including the MAR/intronic (iE_κ) and 3′ enhancers ($3'E_\kappa$). Previous transgenic studies indicate that both κ enhancers are individually necessary for SHM of *Igk*. In contrast, later studies of Ag-selected V_κ genes in $3'E_\kappa^{-/-}$ mice found no absolute requirement for $3'E_\kappa$ in κ SHM. To address the roles of the two κ enhancers in SHM in a physiological context, we analyzed SHM of the endogenous *Igk* in mice with a targeted deletion of either iE_κ or $3'E_\kappa$ in Peyer's patch germinal center B cells. Our findings indicate that, although $3'E_\kappa$ is quantitatively important for SHM of *Igk*, iE_κ is not required for κ SHM. In addition, a reduction of κ mRNA levels is also detected in activated $3'E_\kappa^{-/-}$ B cells. These findings suggest that iE_κ and $3'E_\kappa$ play distinct roles in regulating *Igk* transcription and SHM. ***The Journal of Immunology,*** **2006, 177: 1146–1151.**

B cells diversify the repertoire of their Ag receptor genes through multiple and distinct processes. For example, somatic joining of the V, D, and J gene segments, mediated by the RAGs, occurs during early B cell development (1). In addition, somatic hypermutation (SHM)[4] of the rearranged V(D)J sequence, mediated by the activation-induced deaminase gene (*AID*), occurs in activated B cells in response to antigenic challenge (2). The combinatory effects of SHM and the selection for B cells expressing Ig with a higher affinity for Ag leads to affinity maturation (3). SHM is a tightly regulated process such that mutations are targeted almost exclusively to the rearranged Ig loci, with rare but significant mistargeting to oncogenes (3). However, the mechanism that targets SHM to rearranged Ig loci remains unclear.

Accumulating evidence has identified a connection between SHM and transcription (4). For example, the expression levels of transgenes strongly correlate with the levels of mutation (5–7). In addition, hypermutation of the Ig genes begins just downstream of the promoter (8, 9) and ends well before the C region (10). This ~2-kb window from the promoter for SHM is observed regardless of which J_κ gene segment is rearranged (8, 11). Consistent with the notion that the distance to the promoter determines the mutability of a region, the insertion of a promoter upstream of the C region in a transgenic *Igk* construct caused SHM within the C region at levels similar to the V region (12).

Three enhancers have been identified within the *Igk* locus: one within the intron between $J_\kappa 5$ and C_κ (called the intronic enhancer, or iE_κ) (13), another 9 kb 3′ of C_κ (the 3′ enhancer, or $3'E_\kappa$) (14), and a third 8 kb downstream of $3'E_\kappa$ (the downstream enhancer, or Ed) (15). The deletion of either iE_κ or $3'E_\kappa$ through gene targeting leads to a quantitative decrease in *Igk* rearrangement (16, 17), and a near-complete block in *Igk* rearrangement is observed with the loss of both enhancers, indicating that these two enhancers are collectively essential for *Igk* rearrangement (18).

However, the roles of these enhancers in regulating κ SHM have been more controversial. Transgenic studies indicated that both iE_κ and $3'E_\kappa$ were necessary for the SHM of *Igk* transgenes (19, 20). In this context, deletion of iE_κ or $3'E_\kappa$ resulted in a dramatic reduction of SHM of the V_κ region within *Igk* transgenes to levels equivalent to that caused by PCR error (20). However, analysis of mice bearing a deletion of the endogenous 3′ enhancer leads to a different conclusion. When immunized with the hapten 2-phenyl-5-oxazolone (ph-Ox), $3'E_\kappa^{-/-}$ mice underwent wild-type (Wt) levels of SHM of their V_κ regions, demonstrating that $3'E_\kappa$ is not absolutely required for SHM of *Igk* (21). In addition, the amount of anti-ph-Ox Abs present in the sera of the immunized $3'E_\kappa^{-/-}$ mice was comparable with that of Wt mice. However, in these mice, the SHM of the endogenously rearranged $V_\kappa Ox1/J_\kappa 5$ exon was analyzed after repeated immunization with ph-Ox. Because B cells expressing an Ig_κ with higher avidity to the hapten are selected for survival during Ag-driven affinity maturation, it is possible that the functions of $3'E_\kappa$ in κ SHM might be masked by such stringent selection. In this context, mice with reduced capacity for SHM might still produce B cells with hypermutated Ig_κ. In this regard, it was noted that the mutation frequency of the strong hot spot was potentially decreased in $3'E_\kappa$-deleted loci, leading to the suggestion that the Ag-driven B cell activation and/or somatic mutation might be less efficient in $3'E_\kappa$-deleted cells (21).

In addition to reduced SHM, *Igk* transgenes lacking $3'E_\kappa$ also have dramatically reduced expression (20). Because transcription is closely correlated with the efficiency of SHM, it was hypothesized that the defect in SHM of the $3'E_\kappa$-deleted *Igk* transgene was

*Division of Biological Sciences, University of California, San Diego, La Jolla, CA 92093; and [†]Section of Immunobiology, Howard Hughes Medical Institute, Yale University School of Medicine, New Haven, CT 06510

Received for publication January 28, 2005. Accepted for publication May 1, 2006.

The costs of publication of this article were defrayed in part by the payment of page charges. This article must therefore be hereby marked *advertisement* in accordance with 18 U.S.C. Section 1734 solely to indicate this fact.

[1] This work was supported by National Institutes of Health Grant AI44838 (to Y.X.). D.G.S. is a Howard Hughes Medical Institute investigator.

[2] M.A.I. and H.H.G. contributed equally to this work.

[3] Address correspondence and reprint requests to Dr. Yang Xu, Division of Biological Sciences, University of California, San Diego, 9500 Gilman Drive, La Jolla, CA 92093-0322. E-mail address: yangxu@ucsd.edu

[4] Abbreviations used in this paper: SHM, somatic hypermutation; iE_κ, κ intronic enhancer; $3'E_\kappa$, κ 3′ enhancer; κ, Ig κ L chain; *Igk*, Ig κ L chain locus; ph-Ox, 2-phenyl-5-oxazolone; Wt, wild type; GC, germinal center; PP, Peyer's patch; PNA, peanut agglutinin; SRBC, sheep RBC; iono, inomycin.

0022-1767/06/$02.00

caused by the reduced transcription. In 3′$E_\kappa^{-/-}$ mice, surface expression of *Igk* on mature resting B cells is reduced. However, *Igk* transcription appeared normal in 3′$E_\kappa^{-/-}$ B cells activated by LPS (17). Because stimulation of B cells by LPS involves many pathways but not the ones involved in signaling through the Ag receptor or CD40, it remains to be tested whether 3′E_κ is important for κ transcription during an immune response.

iE_κ plays a quantitatively more important role than 3′E_κ in activating *Igk* rearrangement (18). However, in contrast to 3′$E_\kappa^{-/-}$ B cells, κ expression in $iE_\kappa^{-/-}$ B cells is normal (16). Although transgenic studies have indicated a critical role of iE_κ in SHM of the transgenic *Igk* (20), the physiological roles of iE_κ in SHM of *Igk* remain to be determined. To address these issues, we used a protocol to analyze SHM of *Igk* in germinal center (GC) B cells during a polyclonal immune response. In this context, Peyer's patch (PP) B cells are exposed to continuous antigenic challenge in the gut lumen, and hence undergo robust SHM (22). We also examined splenic GC B cells following immunization with the Ag Sheep RBC (SRBC), which induces a polyclonal response (23–25). Additionally, only mutations within the 5′ end of the $J_\kappa C_\kappa$ intron, which have no bearing on the specificity of the Ab and therefore will not be selected by Ag, were analyzed. Our findings indicate a quantitatively important role for 3′E_κ, but not iE_κ, in κ SHM.

Materials and Methods

Generation of $iE_\kappa^{-/-}$ mice

iE_κ and associated MAR of the endogenous κ allele was replaced with the LoxP-flanked PGK-Neo^r gene in ES cells exactly as previously described (16). The heterozygous mutant ES cells were used to generate chimeric mice that transmitted the mutant allele into germline. To excise the PGK-Neo^r gene from the targeted allele, the germline heterozygous mutant mice with the PGK-Neo^r gene inserted in the targeted allele were bred with CMV-Cre transgenic mice that express the Cre enzyme in zygotes. The resulting heterozygous mutant mice with the PGK-Neo^r gene deleted from the targeted allele were intercrossed to generate homozygous $iE_\kappa^{-/-}$ mice.

Immunizations and splenic and PP GC B cell sorting

PP were harvested from $iE_\kappa^{-/-}$, 3′$E_\kappa^{-/-}$, and Wt littermates. Cells were stained with anti-mouse B220 or CD19 conjugated to PE (BD Pharmingen) and anti-mouse GL7 conjugated to FITC (BD Pharmingen). Live $GL7^-$ and $GL7^+$ B cells were sorted using a FACSVantage cell sorter (BD Biosciences). Alternatively, PP cells were stained with anti-mouse Ig_κ conjugated to PE (BD Pharmingen) and anti-mouse GL7 Abs, and then $Ig_\kappa^+GL7^+$ cells were sorted. 3′$E_\kappa^{-/-}$ and Wt littermates of 5 mo of age were immunized with 2×10^8 SRBC (catalog no. R3378; Sigma-Aldrich). At day 7, mice were given a booster of 2×10^8 SRBC. At day 14, spleens and lymph nodes were collected from these mice and purified into single-cell suspensions, which were stained with anti-mouse B220 (BD Pharmingen) Abs conjugated to PE (BD Pharmingen) and peanut agglutinin (PNA)-FITC (Vector Laboratories). Live (PI^-) $B220^+PNA^{high}$ GC B cells were sorted.

Analysis of SHM

Genomic DNA from sorted cells was purified, and the $J_\kappa C_\kappa$ intron was amplified by PCR using KOD hot-start polymerase (Calbiochem) according to the manufacturer's protocol, with the following primers: V_κD.bam, 5′-ccggatccGGCTGCAGSTTCAGTGGCAGTGGRTCWGGRAC-3′; K1.eco, 5′-ggcgaattcGTGACAAATTTTAGAATAAGAGTCACACCTC-3′.

Sequences in lowercase were added to introduce restriction sites for cloning. The PCR conditions were 95°C for 2 min, followed by 32–35 cycles of 94°C for 20 s, 57°C for 30 s, and 68°C for 1 min, concluding with a final extension at 68°C for 10 min. Purified PCR products were cloned into pBluescript and sequenced. Clones were sequenced using the T3 primer. Sequences were aligned using ClustalX software and scored for mutations. The unpaired *t* test was used. A value of $p < 0.05$ was considered significant.

B cell stimulations and flow cytometry analysis

Single-cell suspensions of spleens from 3′$E_\kappa^{-/-}$ and Wt littermates were stained with microbead-conjugated anti-CD43 Abs (Miltenyi Biotec) and biotinylated anti-Igλ Abs (BD Pharmingen), followed by a secondary stain with microbead-conjugated anti-biotin Abs (Miltenyi Biotec). κ^+ B cells were enriched using the MACS system (Miltenyi Biotec) and were 90–95% pure. Purified κ^+ B cells were cultured in RPMI 1640 medium supplemented with 15% FBS, penicillin/streptomycin, L-glutamine, and 100 mM 2-ME at 10^6 cells/ml, and then stimulated with 10 μg/ml anti-IgM (Jackson ImmunoResearch Laboratories) and 5 μg/ml anti-CD40 (BD Pharmingen) Abs, 50 nM PMA (Calbiochem) and 1 μM ionomycin (Calbiochem), or 10 μg/ml LPS (Sigma-Aldrich). PP cells were stained with PE-conjugated anti-mouse B220, FITC-conjugated PNA, and biotin-conjugated anti-mouse Ig_κ. Biotinylated Ab was revealed with streptavidin-conjugated allophycocyanin.

Real-time quantitative PCR analysis

Unstimulated and stimulated κ^+ B cells from 3′$E_\kappa^{-/-}$ and Wt littermates were harvested, and their RNA was purified, converted to cDNA, and analyzed by real-time PCR as described previously (26). Primers for C_μ and C_κ are as described (26).

The University of California, San Diego, Animal Subjects Committee approved all experiments that involved mice.

Results

Normal Igk *expression in $iE_\kappa^{-/-}$ B cells*

To examine whether *Igk* expression in activated B cells requires iE_κ, κ surface expression on B cells derived from the PP of Wt and $iE_\kappa^{-/-}$ littermates was analyzed by flow cytometry. The B cell activation in PP was similar between Wt and $iE_\kappa^{-/-}$ mice (Fig. 1*A*). In addition, surface Igκ levels were normal in unactivated ($GL7^-$) as well as activated $iE_\kappa^{-/-}$ B cells ($GL7^+$) when compared with those in Wt controls (Fig. 1, *B* and *C*). Because κ gene rearrangement is compromised in $iE_\kappa^{-/-}$ B cells, as published previously (16), knockout mice exhibit a much higher proportion of Igκ-negative (Igλ-positive) cells. Thus, consistent with the conclusion from the transgenic studies (20), iE_κ is not required for κ expression in activated B cells.

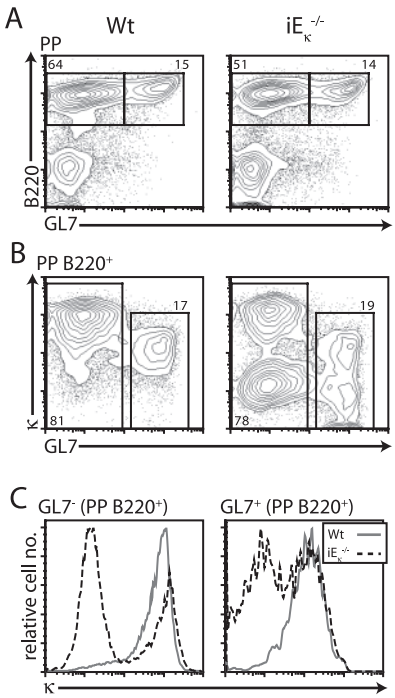

FIGURE 1. κ expression in Wt and $iE_\kappa^{-/-}$ GC and non-GC B cells. *A*, Comparison of the B cell populations in Wt (*right*) and $iE_\kappa^{-/-}$ (*left*) PP. Gates and percentages of non-GC ($GL7^-B220^+$) and GC ($GL7^+B220^+$) B cells are shown. *B*, Comparison of surface κ expression between non-GC and GC B cells. $B220^+$ PP cells are plotted for the surface κ expression and intensity of GL7 staining. *C*, Surface κ expression in non-GC (*left*) and GC (*right*) B cells in Wt (solid gray) and $iE_\kappa^{-/-}$ (dotted black) PP.

Normal κ SHM in $iE_\kappa^{-/-}$ mice

To determine the role of iE_κ in κ SHM, GC κ^+ B cells ($\kappa^+B220^+GL7^+$) were sorted from the pooled PP of three 4-mo-old Wt and $iE_\kappa^{-/-}$ littermates. To amplify only the rearranged *Igk* allele from genomic DNA purified from the sorted B cells, we used the degenerate V_κ primer, which binds to ~90% of V_κ gene segments (27), and a primer ~600 bp downstream of $J_\kappa5$ (Fig. 2*A*). PCR products were cloned into pBluescript and sequenced. Because mutations within the intronic region 3′ of $J_\kappa5$ are not selected by Ag, we analyzed the mutation frequency in the 500-bp intronic sequence. The mutation rate was 12.6×10^{-3} mutations/bp for Wt B cells and 15.8×10^{-3} for the $iE_\kappa^{-/-}$ B cells (Fig. 2*B* and Table I). Although κ SHM appeared slightly elevated in $iE_\kappa^{-/-}$ B cells, this was due to the lower number of sequences analyzed with zero mutations, because the mutation frequency on sequences containing at least one mutation was equivalent between $iE_\kappa^{-/-}$ and Wt (Table I). The mutational spectra were also similar between Wt and $iE_\kappa^{-/-}$ B cells (Fig. 2*C*), resulting in similar percentages of transitions and transversions (Table I). The mutations identified from both groups showed the hallmarks of mutations generated by SHM, because they were RGYW/WRCY hot spot targeted and biased toward transitions (Table I). Thus, κ SHM is normal in $iE_\kappa^{-/-}$ mice.

Reduced κ mRNA levels in activated $3'E_\kappa^{-/-}$ B cells

Because deletion of $3'E_\kappa$ leads to a reduction in κ surface expression in unactivated B cells (17), we examined how κ expression is affected in activated $3'E_\kappa^{-/-}$ B cells. Previous studies indicated that $3'E_\kappa$ was not necessary for κ expression in B cells activated by LPS (17). However, because LPS activates B cells independently of the BCR, we analyzed κ mRNA levels in Wt and $3'E_\kappa^{-/-}$ B cells activated in vitro by multiple stimuli using real-time PCR. Consistent with earlier findings, there was a ~3-fold decrease in κ mRNA levels in resting $3'E_\kappa^{-/-}$ B cells when compared with that

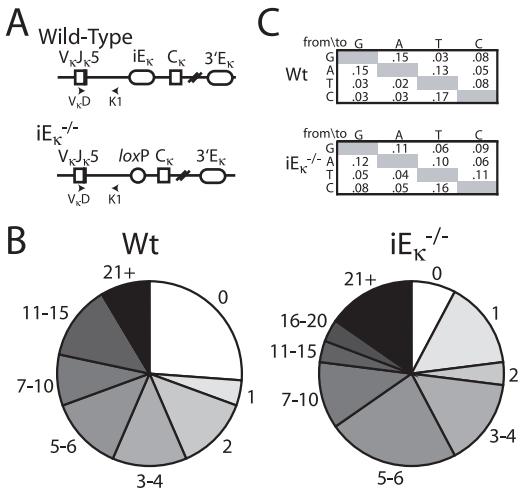

FIGURE 2. κ SHM in pooled PP κ^+ GC B cells of three pairs of 4-mo-old Wt and $iE_\kappa^{-/-}$ littermates. *A*, PCR strategy for detecting SHM. Genomic DNA from purified GC B cells was amplified by PCR using the degenerate V_κ primer and the K1 primer, which anneals ~700 bp downstream of $J_\kappa5$. *B*, Pie chart of κ SHM in Wt (*left*) and $iE_\kappa^{-/-}$ (*right*) samples. Each pie slice represents the proportion of sequences containing the number of mutations listed on the perimeter. *C*, Mutation spectrum of κ in Wt and $iE_\kappa^{-/-}$ PP GC B cells. The nucleotides listed on the *y*-axis represent the germline nucleotide, and the nucleotide on the *x*-axis shows the mutation. The proportions of each type of substitution are displayed in the chart, adjusted for the percentage of each type of nucleotide in the 500-bp sequence analyzed (G, 28.2%; A, 31.6; T, 26.4%; C, 13.8%).

Table I. *SHM of the κ intronic region in Wt and $iE_\kappa^{-/-}$ GC B cells*

	PP	
	Wt	$iE_\kappa^{-/-}$
No. of sequences	23	26
Total point mutations	145	206
Mutation frequency 1[a]	12.6×10^{-3}	15.8×10^{-3}
Mutation frequency 2[b]	17.0×10^{-3}	17.2×10^{-3}
RGYW/WRCY mutations (%)	34	41
Transition mutations (%)	58	49

[a] Mutation frequency 1 was calculated as follows: number of total mutations/total number of base pairs analyzed for all sequences scored.
[b] Mutation frequency 2 was calculated with only those sequences that contained at least one mutation.

in resting Wt B cells (17) (Fig. 3*A*). In addition, similar levels of κ expression were detected between $3'E_\kappa^{-/-}$ and Wt B cells stimulated with LPS (Fig. 3*A*). However, when stimulated with anti-IgM and anti-CD40 Abs that mimic B cell activation during an immune response, a ~3-fold reduction in κ mRNA levels was detected in $3'E_\kappa^{-/-}$ B cells when compared with that in Wt B cells (Fig. 3*A*). Because the lower surface expression of IgM in $3'E_\kappa^{-/-}$ B cells might affect the signaling through the BCR, we treated B cells with PMA and ionomycin, which directly activate signaling pathways downstream of the BCR independent of BCR engagement. κ mRNA levels were 5-fold lower in $3'E_\kappa^{-/-}$ B cells than in Wt B cells after stimulation with PMA/ionomycin (Fig. 3*A*). The differences in κ mRNA levels also resulted in analogous differences in κ surface expression in the activated B cells (Fig. 3*B*). To further ensure that the reduced transcription in activated $3'E_\kappa^{-/-}$ B cells is not due to impaired activation, we compared the activation efficiency between Wt and $3'E_\kappa^{-/-}$ B cells under each of the stimulation conditions. The percentage of activated B cells, which express the early activation marker CD69 and are actively dividing, were similar between $3'E_\kappa^{-/-}$ and Wt B cells after various stimulations (Fig. 3*B*).

To examine κ mRNA levels in activated B cells in vivo, we sorted κ^+ GC B cells from the PP of five pairs of Wt and $3'E_\kappa^{-/-}$ littermates. The mRNA levels of κ were ~2-fold reduced in $3'E_\kappa^{-/-}$ GC B cells than in Wt GC B cells (Fig. 4*A*). However, when the total PP B cells were analyzed by flow cytometry, κ surface expression in $3'E_\kappa^{-/-}$ GC B cells was only slightly lower than Wt (Fig. 4*B*). This is caused in part by the reduction of surface IgM in activated GC B cells ($B220^+PNA^{high}$) compared with non-GC B cells (28, 29) (Fig. 4*C*), likely as a result of a reduction in C_μ mRNA levels in the $B220^+PNA^{high}$ GC B cells (Fig. 4*D*). The lower κ mRNA levels are not due to a defect in B cell activation, because the proportion of activated B cells (Fig. 4*E*), or specifically activated κ^+ B cells (Fig. 4*C*), is similar between the PP of $3'E_\kappa^{-/-}$ and Wt mice. When compared with that in $3'E_\kappa^{-/-}$ B cells stimulated by PMA and ionomycin in vitro, the reduction of κ mRNA levels in $3'E_\kappa^{-/-}$ GC B cells vs Wt controls is less dramatic, likely due to that the constant stimuli of PP B cells include LPS present on the bacterial flora.

Quantitative decrease in κ SHM in $3'E_\kappa^{-/-}$ GC B cells

Although $3'E_\kappa$ was essential for the SHM of an *Igk* transgene, analysis of Ag-driven SHM of *Igk* in $3'E_\kappa^{-/-}$ mice indicated that $3'E_\kappa$ is not required for κ SHM (20, 21). However, it remains possible that $3'E_\kappa$ could still have an influence on overall efficiency of κ SHM. Additionally, given the correlation between SHM and transcription efficiency, the reduction in κ mRNA levels we observed in $3'E_\kappa^{-/-}$ GC B cells suggests the possibility of a

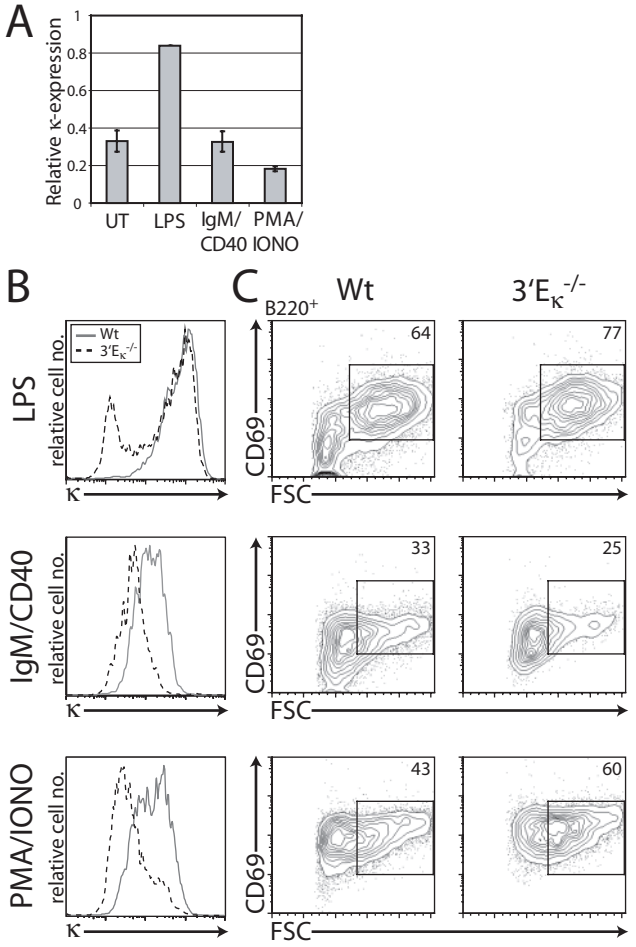

FIGURE 3. Analysis of κ expression in stimulated Wt and 3′$E_\kappa^{-/-}$ B cells. *A*, Ratio of κ mRNA levels in stimulated 3′$E_\kappa^{-/-}$ B cells vs those in stimulated Wt B cells. κ^+ B cells were purified by MACS and activated by a variety of stimuli. Untreated (UT) B cells were harvested immediately after sorting, and stimulated B cells were harvested 2 days after stimulation. Quantitative real-time PCR using primers specific for the κ and μ C regions was used to analyze the gene expression of κ and μ, respectively. All samples were normalized to C_μ expression. *B*, κ surface expression profile in stimulated Wt (solid gray) and 3′$E_\kappa^{-/-}$ (dotted black) B cells. Only cells within the gates displayed in Fig. 3*C* are shown. *C*, Analysis of the activation efficiency in 3′$E_\kappa^{-/-}$ and Wt B cells by flow cytometry. Samples from each type of stimulation were stained with anti-B220, -CD69, and -κ Abs. CD69 expression (*y*-axis) and cell size (*x*-axis) of live, $B220^+$ lymphocytes are shown. The percentage of $CD69^+$, blasting Wt (*left column*) and 3′$E_\kappa^{-/-}$ (*right column*) B cells are listed inside the corresponding gate. IONO, Ionomycin.

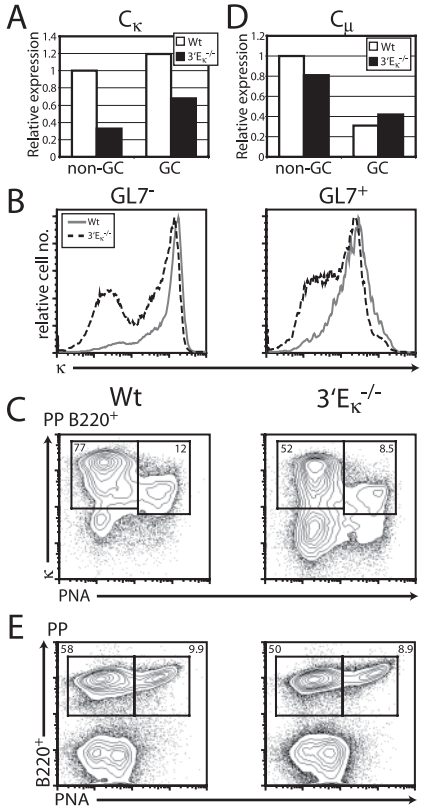

FIGURE 4. κ expression in Wt and 3′$E_\kappa^{-/-}$ PP B cells. *A*, Analysis of κ mRNA levels in κ^+ Wt (□) and 3′$E_\kappa^{-/-}$ (■) PP GC ($GL7^+$) and non-GC ($GL7^-$) B cells. mRNA levels were normalized to CD19 mRNA levels. κ mRNA levels of all samples are shown relative to Wt non-GC sample. *B*, κ surface expression profile of non-GC (*left*) and GC (*right*) B cells of Wt (solid gray) and 3′$E_\kappa^{-/-}$ (dotted black) PP. *C*, Comparison of κ surface expression in PP B cells in 3′$E_\kappa^{-/-}$ and Wt mice. Total $B220^+$ PP cells were plotted for surface κ expression and intensity of PNA staining. *D*, Analysis of C_μ mRNA levels in $B220^+PNA^{high}$ GC B cells. Samples were normalized to CD19 mRNA levels and are shown relative to Wt non-GC. *E*, Proportions of non-GC ($B220^+PNA^{low}$) and GC ($B220^+PNA^{high}$) in Wt (*left*) and 3′$E_\kappa^{-/-}$ (*right*) PP. Gates and percentages of GC and non-GC B cells are shown.

defect in κ SHM in these cells. To address this possibility, we re-examined SHM in 3′$E_\kappa^{-/-}$ mice by analyzing mutations within the $J_\kappa C_\kappa$ intron in GC B cells after immunization with SRBCs. Five-month-old Wt and 3′$E_\kappa^{-/-}$ littermates were immunized with 2×10^8 SRBCs, and then given a booster injection at day 7. At day 14, spleen cells were purified, stained with an Ab for the B cell marker B220, and with PNA, which stains brightly for GC B cells, and GC B cells ($B220^+$, PNA^{high}) were sorted. Genomic DNA from these GC B cells was purified, and $V_\kappa J_\kappa 5$ rearrangements were amplified by PCR, cloned, and sequenced. In Wt GC B cells, we detected an average of 3.7 mutations per 500 bp of sequence in the samples (7.3×10^{-3} mutations per base) (Table II and Fig. 5*A*). In contrast, only 1.3 mutations per 500 bp were detected in sequences derived from 3′$E_\kappa^{-/-}$ GC B cells (2.6×10^{-3} per base), an ~3-fold reduction. Furthermore, the number of unmutated sequences was ~2.5-fold greater in 3′$E_\kappa^{-/-}$ GC B cells (51%) compared with Wt (18%) (Fig. 5*A*). This did not fully account for the SHM defect, because the average number of mutations on sequences containing at least one mutation was still 2-fold reduced in 3′$E_\kappa^{-/-}$ GC B cells, compared with Wt (Table II). The mutation spectrum was similar between Wt and 3′$E_\kappa^{-/-}$ splenic GC B cells (Fig. 5*B*), and displayed equivalent percentages of hot-spot mutations and transitions (Table II).

To confirm the defect in *Igk* SHM observed in 3′$E_\kappa^{-/-}$ splenic GC B cells, we also examined SHM in GC B cells from PP of 6-mo-old unimmunized mice. GC B cells ($CD19^+GL7^+$) were purified from the PP, and the $J_\kappa C_\kappa$ intronic region was sequenced (Fig. 5*C*). In Wt GC B cells, the mutation frequency of the analyzed region was 16×10^{-3} (Table II). However, in 3′$E_\kappa^{-/-}$ GC B cells, the mutation frequency was reduced 2.5-fold. The same proportion of sequences contained mutations in both groups, but the sequences from 3′$E_\kappa^{-/-}$ GC B cells had a lower mutation load than the Wt. Wt and 3′$E_\kappa^{-/-}$ B cells show a similar spectrum of mutations (data not shown). Additionally, the mutations analyzed from both groups are targeted to RGYW/WRCY hotspots and transition biased (Table II). The variation in the mutational frequency

Table II. *SHM of the κ intronic region in Wt and $3'E_\kappa^{-/-}$ GC B cells*

	Spleen		PP		PP (κ^+ only)	
	Wt	$3'E_\kappa^{-/-}$	Wt	$3'E_\kappa^{-/-}$	Wt	$3'E_\kappa^{-/-}$
No. of sequences	33	45	32	30	24	31
Total point mutations	121	59	296	97	268	152
Mutation frequency 1[a]	7.3×10^{-3}	2.6×10^{-3}*	16×10^{-3}	6×10^{-3}*	22×10^{-3}	9.8×10^{-3}*
Mutation frequency 2[b]	9.0×10^{-3}	5.4×10^{-3}*	19×10^{-3}	7×10^{-3}*	22×10^{-3}	14×10^{-3}
RGYW/WRCY mutations (%)	44	43	50	51	ND	ND
Transition mutations (%)	50	48	55	64	ND	ND

[a] Mutation frequency 1 was calculated as follows: number of total mutations/total number of base pairs analyzed for all sequences scored.
[b] Mutation frequency 2 was calculated with only those sequences that contained at least one mutation.
*, $p < 0.05$ (unpaired t test).

in the Wt GC B cells between different experiments was likely due to the different ages of mice analyzed, because older mice accumulate more mutations in *Igk* of GC B cells.

Although the sorted GC cells in the previous two experiments included λ^+ B cells, which are a significant population in $3'E_\kappa^{-/-}$ mice, we would not expect that these λ^+ B cells contribute to the SHM data, because the rearranged *Igk* loci are mostly deleted through RS rearrangement in $3'E_\kappa^{-/-}$ λ^+ B cells (17). However, to rule out the possibility that a larger proportion of λ^+ B cells in sorted GC B cells could lead to skewed data, we repeated the analysis of sorted κ^+ GC cells (κ^+GL7^+) from the PP of 6-mo-old Wt and $3'E_\kappa^{-/-}$ littermates. In Wt and $3'E_\kappa^{-/-}$ GC κ^+ B cells, the mutation frequencies of the analyzed region were 22×10^{-3} and 10×10^{-3}, respectively, a 2.2-fold difference (Fig. 5*D*, Table II). Therefore, $3'E_\kappa$ is quantitatively important for κ SHM.

Discussion

Recruitment of the SHM machinery specifically to the rearranged Ig loci is critical for Ab maturation as well as the maintenance of genetic stability via the prevention of hypermutation in other parts of the genome. *cis*-elements within the Ig loci have been thought to play critical roles in this recruitment process. Transgenic studies implicated essential roles for both iE_κ and $3'E_\kappa$ in driving κ SHM (20). In this study, we report the first analysis of SHM of the endogenous *Igk* allele in the absence of iE_κ. In contrast with the findings of the transgenic studies (20), we have observed no apparent defect in κ SHM in $iE_\kappa^{-/-}$ mice. Given the very small size of transgenes compared with the endogenous 3.2-Mb *Igk* locus, the discrepancy is likely due to the presence of other *cis*-elements that play redundant roles in activating κ SHM. One potential candidate is the recently discovered downstream enhancer (Ed), which was not contained in the κ transgenes (15).

Previous studies of the functions of $3'E_\kappa$ in κ SHM have reached conflicting conclusions regarding its importance. Transgenic studies indicated that $3'E_\kappa$ is critical for the expression and SHM of *Igk* in randomly integrated transgenes in the presence as well as absence of stringent Ag selection (20, 30). However, analyses of $3'E_\kappa^{-/-}$ mice showed that $3'E_\kappa$ is not important for κ transcription following LPS-induced activation (17) and also that $3'E_\kappa$ is not required for Ag-driven SHM (21). However, these authors noted a potentially reduced mutation frequency and proposed that $3'E_\kappa$ might be involved in promoting the optimal efficiency of κ SHM. By analyzing SHM in the $J_\kappa C_\kappa$ intron following immunization with the polyclonal response-inducing Ag SRBC, or in unimmunized PP, we confirm that the $3'E_\kappa$ is indeed not required for κ SHM. However, our findings clearly demonstrate that $3'E_\kappa$ is quantitatively important for κ SHM.

Because of the correlation between transcription and SHM, we analyzed κ mRNA levels in $3'E_\kappa^{-/-}$ B cells activated by a number of stimuli. Consistent with earlier observations (17), normal κ mRNA levels are observed in $3'E_\kappa^{-/-}$ B cells activated by LPS. However, κ expression appears to be impaired in $3'E_\kappa^{-/-}$ B cells

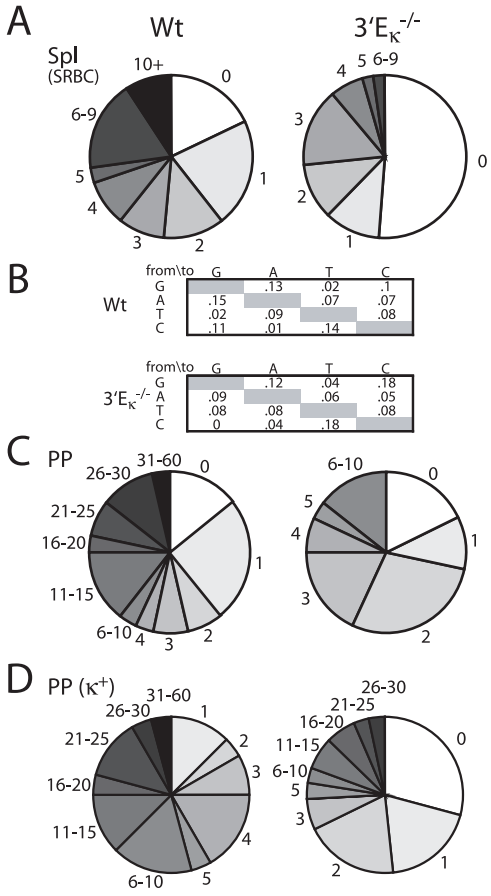

FIGURE 5. Analysis of κ SHM in GC B cells of Wt and $3'E_\kappa^{-/-}$ mice. *A*, Pie chart of κ SHM in splenic GC B cells of 5-mo-old Wt and $3'E_\kappa^{-/-}$ littermates after SRBC immunization. Each pie slice represents the proportion of sequences containing the number of mutations indicated on the perimeter of each slice. The data are pooled from three pairs of immunized Wt and $3'E_\kappa^{-/-}$ littermates. *B*, Mutation spectrum of κ in Wt and $3'E_\kappa^{-/-}$ splenic GC B cells. The nucleotides listed on the *y*-axis represent the germline nucleotide, and the nucleotide on the *x*-axis shows the mutation. The proportions of each type of substitution are displayed in the chart, adjusted for the percentage of each type of nucleotide in the 500-bp sequence analyzed (G, 28.2%; A, 31.6%; T, 26.4%; C, 13.8%). *C*, Pie chart of κ SHM in pooled PP GC B cells of 6-mo-old Wt and $3'E_\kappa^{-/-}$ mice. Each slice represents the proportion of the sequences with the number of mutations listed on the perimeter. *D*, Pie chart of κ SHM in pooled κ^+ GC B cells of four pairs of 6-mo-old Wt and $3'E_\kappa^{-/-}$ mice.

when signaling pathways downstream of the BCR and CD40 are activated. We therefore conclude that $3'E_\kappa$, similar to its function in developing and mature B cells, is an important mediator of κ transcription in activated B cells. The surface κ expression of Wt and $3'E_\kappa^{-/-}$ GC B cells is similar, possibly due to reduced *IgH* transcription in GC B cells. Therefore, the modest defect in κ transcription, but not surface expression, observed in $3'E_\kappa^{-/-}$ GC B cells could explain the reduced mutation of *Igk* in $3'E_\kappa^{-/-}$ mice.

Our findings that neither $3'E_\kappa$ nor iE_κ is critical for κ SHM suggest that these two enhancers might play redundant roles in activating κ SHM. A similar scenario has been observed in the regulation of *Igk* rearrangement by the two enhancers (18). Furthermore, mice bearing a deletion of the core region of the *IgH* E_μ enhancer show no defect in SHM of *IgH* (31). E_μ can drive a low level of SHM in transgenic constructs (32–34), but not others (35, 36), implicating a role for multiple elements in the regulation of SHM at the *IgH* locus.

Transcription factors binding to the enhancer elements might be involved in SHM recruitment. In this context, two accidentally introduced E2A binding sites, in addition to those already present in iE_κ and $3'E_\kappa$, were found to increase SHM in a κ transgene with no apparent impact on the transcription of the κ transgene (25). As both iE_κ and $3'E_\kappa$ contain E2A binding sites, these enhancers might activate SHM via the recruitment of E2A. iE_κ's two E2A binding sites have been shown to be important for *Igk* rearrangement (26). Therefore, similar to their redundant roles in the regulation of κ rearrangement, the intronic and 3′ enhancers might play redundant roles in activating κ SHM (18). Targeted replacement of J_κ with a rearranged $V_\kappa J_\kappa$ driven by a constitutive promoter in the context of an enhancerless *Igk* allele might reveal the redundant roles of the two *Igk* enhancers in targeting SHM to *Igk* loci.

Acknowledgments

We thank Drs. Mark Schlissel and Fred Alt for the $3'E_\kappa^{-/-}$ mice, and Dr. Fred Alt for critical reading of the manuscript.

Disclosures

The authors have no financial conflict of interest.

References

1. Bassing, C. H., W. Swat, and F. W. Alt. 2002. The mechanism and regulation of chromosomal V(D)J recombination. *Cell* 109: S45–S55.
2. Honjo, T., K. Kinoshita, and M. Muramatsu. 2002. Molecular mechanism of class switch recombination: linkage with somatic hypermutation. *Annu. Rev. Immunol.* 20: 165–196.
3. Wagner, S. D., and M. S. Neuberger. 1996. Somatic hypermutation of immunoglobulin genes. *Annu. Rev. Immunol.* 14: 441–457.
4. Storb, U., A. Peters, E. Klotz, N. Kim, H. M. Shen, K. Kage, B. Rogerson, and T. E. Martin. 1998. Somatic hypermutation of immunoglobulin genes is linked to transcription. *Curr. Top. Microbiol. Immunol.* 229: 11–19.
5. Goyenechea, B., N. Klix, J. Yelamos, G. T. Williams, A. Riddell, M. S. Neuberger, and C. Milstein. 1997. Cells strongly expressing Igκ transgenes show clonal recruitment of hypermutation: a role for both MAR and the enhancers. *EMBO J.* 16: 3987–3994.
6. Fukita, Y., H. Jacobs, and K. Rajewsky. 1998. Somatic hypermutation in the heavy chain locus correlates with transcription. *Immunity* 9: 105–114.
7. Bachl, J., C. Carlson, V. Gray-Schopfer, M. Dessing, and C. Olsson. 2001. Increased transcription levels induce higher mutation rates in a hypermutating cell line. *J. Immunol.* 166: 5051–5057.
8. Lebecque, S. G., and P. J. Gearhart. 1990. Boundaries of somatic mutation in rearranged immunoglobulin genes: 5′ boundary is near the promoter, and 3′ boundary is approximately 1 kb from V(D)J gene. *J. Exp. Med.* 172: 1717–1727.
9. Rada, C., A. Gonzalez-Fernandez, J. M. Jarvis, and C. Milstein. 1994. The 5′ boundary of somatic hypermutation in a V κ gene is in the leader intron. *Eur. J. Immunol.* 24: 1453–1457.
10. Hackett, J., Jr., B. J. Rogerson, R. L. O'Brien, and U. Storb. 1990. Analysis of somatic mutations in κ transgenes. *J. Exp. Med.* 172: 131–137.
11. Weber, J. S., J. Berry, T. Manser, and J. L. Claflin. 1991. Position of the rearranged Vκ and its 5′ flanking sequences determines the location of somatic mutations in the Jκ locus. *J. Immunol.* 146: 3652–3655.
12. Peters, A., and U. Storb. 1996. Somatic hypermutation of immunoglobulin genes is linked to transcription initiation. *Immunity* 4: 57–65.
13. Queen, C., and D. Baltimore. 1983. Immunoglobulin gene transcription is activated by downstream sequence elements. *Cell* 33: 741–748.
14. Meyer, K. B., and M. S. Neuberger. 1989. The immunoglobulin kappa locus contains a second, stronger B-cell-specific enhancer which is located downstream of the constant region. *EMBO J.* 8: 1959–1964.
15. Liu, Z.-M., J. B. George-Raizen, S. Li, K. C. Meyers, M. Y. Chang, and W. T. Garrard. 2002. Chromatin structural analyses of the mouse Igκ gene locus reveal new hypersensitive sites specifying a transcriptional silencer and enhancer. *J. Biol. Chem.* 277: 32640–32649.
16. Xu, Y., L. Davidson, F. W. Alt, and D. Baltimore. 1996. Deletion of the Ig κ light chain intronic enhancer/matrix attachment region impairs but does not abolish Vκ Jκ rearrangement. *Immunity* 4: 377–385.
17. Gorman, J. R., N. vanderStoep, R. Monroe, M. Cogne, L. Davidson, and F. W. Alt. 1996. The Ig κ 3′ enhancer influences the ratio of Ig κ versus Ig λ B lymphocytes. *Immunity* 5: 241–252.
18. Inlay, M., F. W. Alt, D. Baltimore, and Y. Xu. 2002. Essential roles of the κ light chain intronic enhancer and 3′ enhancer in κ rearrangement and demethylation. *Nat. Immunol.* 3: 463–468.
19. Sharpe, M. J., M. Neuberger, R. Pannell, M. A. Surani, and C. Milstein. 1990. Lack of somatic mutation in a κ light chain transgene. *Eur. J. Immunol.* 20: 1379–1385.
20. Betz, A. G., C. Milstein, A. Gonzalez-Fernandez, R. Pannell, T. Larson, and M. S. Neuberger. 1994. Elements regulating somatic hypermutation of an immunoglobulin κ gene: critical role for the intron enhancer/matrix attachment region. *Cell* 77: 239–248.
21. van der Stoep, N., J. R. Gorman, and F. W. Alt. 1998. Reevaluation of 3′Eκ function in stage- and lineage-specific rearrangement and somatic hypermutation. *Immunity* 8: 743–750.
22. Gonzalez-Fernandez, A., D. Gilmore, and C. Milstein. 1994. Age-related decrease in the proportion of germinal center B cells from mouse Peyer's patches is accompanied by an accumulation of somatic mutations in their immunoglobulin genes. *Eur. J. Immunol.* 24: 2918–2921.
23. Rogerson, B. J. 1995. Somatic hypermutation of VHS107 genes is not associated with gene conversion among family members. *Int. Immunol.* 7: 1225–1235.
24. Kim, N., G. Bozek, J. C. Lo, and U. Storb. 1999. Different mismatch repair deficiencies all have the same effects on somatic hypermutation: intact primary mechanism accompanied by secondary modifications. *J. Exp. Med.* 190: 21–30.
25. Michael, N., H. M. Shen, S. Longerich, N. Kim, A. Longacre, and U. Storb. 2003. The E box motif CAGGTG enhances somatic hypermutation without enhancing transcription. *Immunity* 19: 235–242.
26. Inlay, M. A., H. Tian, T. Lin, and Y. Xu. 2004. Important roles for E protein binding sites within the immunoglobulin κ chain intronic enhancer in activating Vκ Jκ rearrangement. *J. Exp. Med.* 200: 1205–1211.
27. Schlissel, M. S., and D. Baltimore. 1989. Activation of immunoglobulin κ gene rearrangement correlates with induction of germline κ gene-transcription. *Cell* 58: 1001–1007.
28. Butcher, E. C., R. A. Reichert, R. L. Coffman, C. Nottenburg, and I. L. Weissman. 1982. Surface phenotype and migratory capability of Peyer's patch germinal center cells. *Adv. Exp. Med. Biol.* 149: 765–772.
29. Butcher, E. C., R. V. Rouse, R. L. Coffman, C. N. Nottenburg, R. R. Hardy, and I. L. Weissman. 1982. Surface phenotype of Peyer's patch germinal center cells: implications for the role of germinal centers in B cell differentiation. *J. Immunol.* 129: 2698–2707.
30. Sharpe, M. J., C. Milstein, J. M. Jarvis, and M. S. Neuberger. 1991. Somatic hypermutation of immunoglobulin κ may depend on sequences 3′ of Cκ and occurs on passenger transgenes. *EMBO J.* 10: 2139–2145.
31. Perlot, T., F. W. Alt, C. H. Bassing, H. Suh, and E. Pinaud. 2005. Elucidation of IgH intronic enhancer functions via germ-line deletion. *Proc. Natl. Acad. Sci. USA* 102: 14362–14367.
32. Azuma, T., N. Motoyama, L. E. Fields, and D. Y. Loh. 1993. Mutations of the chloramphenicol acetyl transferase transgene driven by the immunoglobulin promoter and intron enhancer. *Int. Immunol.* 5: 121–130.
33. Sohn, J., R. M. Gerstein, C. L. Hsieh, M. Lemer, and E. Selsing. 1993. Somatic hypermutation of an immunoglobulin mu heavy chain transgene. *J. Exp. Med.* 177: 493–504.
34. Klotz, E. L., and U. Storb. 1996. Somatic hypermutation of a λ2 transgene under the control of the λ enhancer or the heavy chain intron enhancer. *J. Immunol.* 157: 4458–4463.
35. Hackett, J., Jr., C. Stebbins, B. Rogerson, M. M. Davis, and U. Storb. 1992. Analysis of a T cell receptor gene as a target of the somatic hypermutation mechanism. *J. Exp. Med.* 176: 225–231.
36. Hengstschlager, M., M. Williams, and N. Maizels. 1994. A λ1 transgene under the control of a heavy chain promoter and enhancer does not undergo somatic hypermutation. *Eur. J. Immunol.* 24: 1649–1656.